CFD PREDICTION OF THE INLET NOZZLE VELOCITY PROFILES FOR THE CANDU MODERATOR ANALYSIS

Churl Yoon and Joo Hwan Park

Korea Atomic Energy Research Institute
150 Dukjin-Dong, Yusong-Gu, Daejeon 305-353, Korea
Phone: +82-42-868-2128, Fax: +82-42-868-8590, E-mail: cyoon@kaeri.re.kr

Abstract

For predicting the inlet velocity profile at the CANDU-6 moderator nozzles, a commercial CFD code was tested and applied. The fluid flows going through the moderator piping network have three sections, which are characterized as a straight pipe flow, a curved pipe flow, and an impinging jet, respectively. Some experimental data were chosen for each flow, and various turbulence models were tested and optimized. As a result of the investigation, detailed velocity profiles and turbulent parameters at the nozzle outlets were obtained, which could be used as inlet boundary conditions in the CANDU moderator analysis.

Key Words : CANDU, Curved Pipe, Impinging Jet, Moderator, Nozzle, Pipe Flow

1. INTRODUCTION

For the moderator analysis of the four operating CANDU reactors in Korea, predicting local moderator subcooling in the Calandria vessels is one of the main concerns for assuring fuel channel integrity under LOCA transients. The moderator circulation pattern is determined by the combined forces of the inlet jet momentum and the buoyancy flow. Because the inlet boundary condition plays an important role in determining the moderator circulations, it is essential for the moderator analysis to get the detailed inlet velocity profiles at the nozzles. The purposes of this study are to estimate an analytic CFD tool for predicting the internal flow of the moderator inlet nozzle assembly, and to produce the velocity profiles at the inlet nozzles by a CFD simulation.

The inlet nozzle geometry consists of a circular pipe, a 90^{o} circular bend, and a nozzle as shown in Fig. 1. The whole domain is divided into three separated flow regions, which are characterized as a straight pipe flow, a curved pipe flow, and an impinging jet, respectively. To produce the velocity vector fields at the inlet nozzle surfaces, the internal flows in the nozzle assembly were simulated by using a commercial CFD code, CFX-5.7. In the following section, the analytical capability of CFX-5.7 was estimated by a validation of the CFD code against available experimental data for each flow. Various turbulence models and grid spacing were also tested. In section 3, the inlet nozzle flow through the real nozzle assembly was predicted by using the obtained technique of the CFD simulation.

Fig. 1 An inlet nozzle assembly of the CANDU moderator circulation system

2. VALIDATION OF CFX-5.7

2.1 Internal Pipe Flow

The experimental data of Laufer et al.[2] was selected for the validation of the internal pipe flow. The five turbulence models provided in CFX-5.7 are compared in Figs. 2 & 3. The low-Re near-wall formulation was applied for the k-ω model, the Baseline k-ω model, and the SST k-ω Based model. The mesh for these turbulence models had 6,900 cells in the r-θ plane, and the near wall y^+ value cells were ~0.6. A wall function was applied for the standard k-ε model and the SSG model, in which the mesh has 2,400 cells in the r-θ plane and the near wall y^+ values were ~12.0. Grid independency was confirmed. The flow was fully-developed and the Reynolds number was 40,000. All the turbulent models show a good agreement with the experimental data except f or the abrupt change of the turbulent kinetic energy at the edge of the inner boundary layer (y+ = ~10)..

To overcome the difficulties in predicting the large velocity gradients near the walls of the turbulent flow, a wall function or a low-Re near-wall formulation was used. Figure 4 shows the validation of the wall function and the near-wall treatment. For the case of the circular pipe flows, the wall function and the constants in the logarithmic region are as follows.

$$u^+\left(\equiv\frac{U-U_{wall}}{u_\tau}\right)=\frac{1}{\kappa}\ln y^+ + B \qquad (1)$$

where $y^+ = \dfrac{yu_\tau}{\nu}$, $u_\tau = \sqrt{\dfrac{\tau_w}{\rho}}$,

κ = 0.4 and B = 5.5.

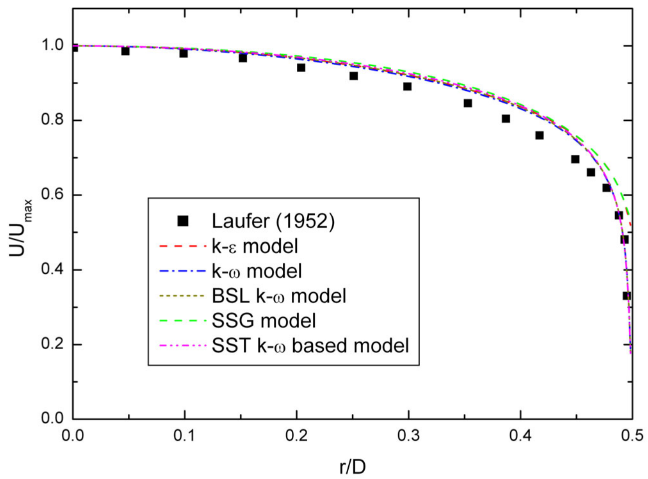

Fig. 2 U Velocity Profile of the Pipe Flow at *Re* = 40,000

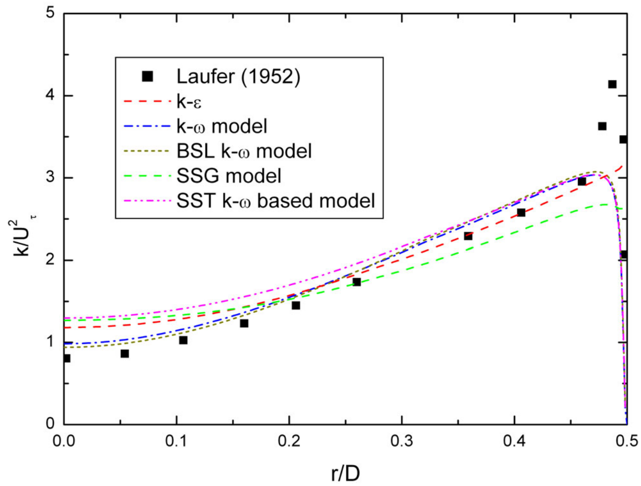

Fig. 3 *k* Profile of the Pipe Flow at *Re* = 40,000

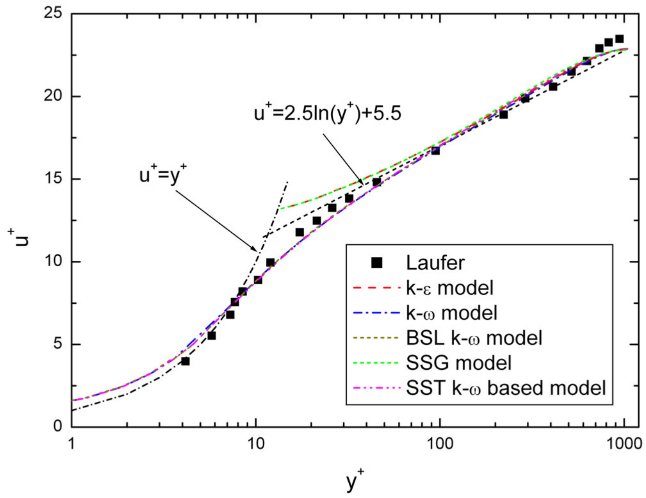

Fig. 4 Semi-log Plot of the Velocity of the Pipe Flow at Re = 40,000

2.2 Curved Pipe Flow

For validation of the CFX-5.7 to predict curved pipe flows, the experimental data of non-swirling fluid flows in a curved pipe by Azzola[3] was selected. The Re number of these experiments was 57,400, and the working fluid was water at 20^{o}C. The measured bulk velocity (U_b) was 1.29 ± 0.03m/s. The schematic of the test section is shown in Fig. 5. Figure 6 shows the comparison of the longitudinal (U) and circumferential (V) mean velocity components and the circumferential turbulent intensity component at sequential longitudinal stations along the flow, in a comparison with the experimental data. The negative sign of X/D indicates the upstream side of the straight tangents, which are connected to the 180^{o} curved pipe. By testing the various turbulence models, it was proven that the Reynolds stress turbulence model developed by Speziale, Sarkar and Gatski[4] (the SSG model) predicted the fluid flow inside a curved pipe relatively well.

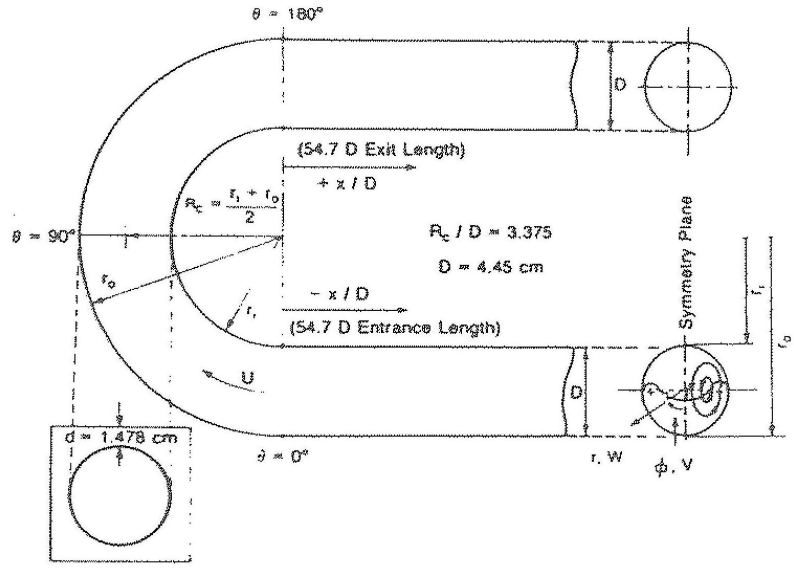

Fig. 5 Test Section Configuration and Coordinate System (from Azzola[3])

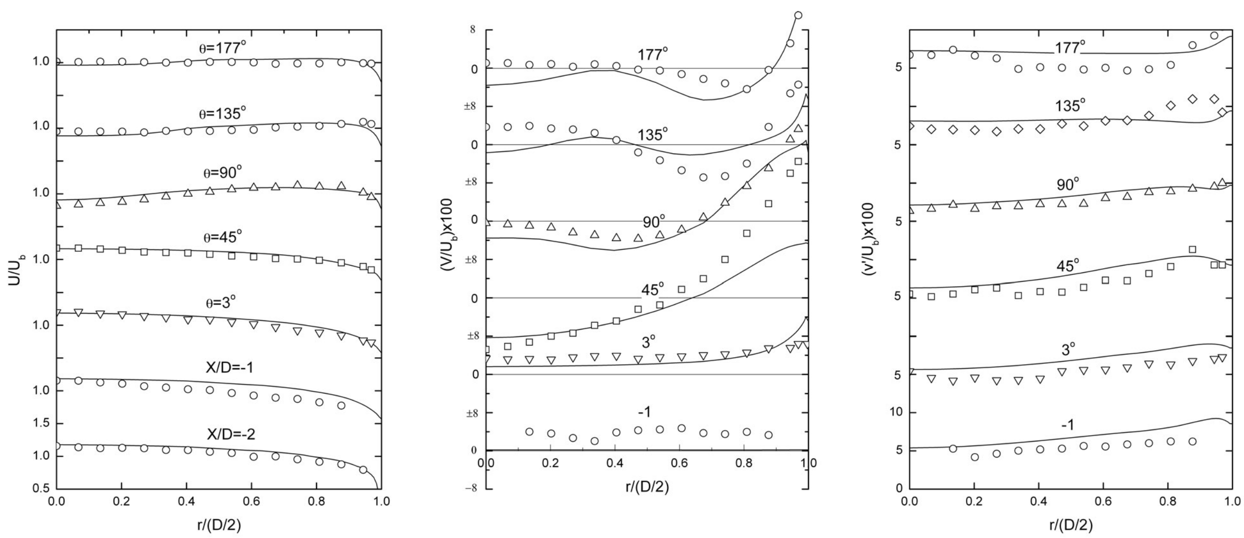

(a) Longitudinal Mean Velocity (U)

(b) Circumferential Mean Velocity (V)

(c) Circumferential Turbulence Intensity Component

Fig. 6 Simulation of the Curved Pipe Flow with the SSG Turbulent Model (with Azzola[3])

2.3 Impinging Jet

A normally-impinging jet from a circular nozzle is simulated and the results are compared with the experimental data by Cooper[5]. A turbulent air jet impinges orthogonally onto a large plane surface. The *Re* number at the nozzle is 70,000. The nozzle diameter D is 101.6 mm and the height of the jet discharge is 2D. The flow at the nozzle was fully-developed. As shown in Fig. 7, the Shear Stress Transport (SST) k-ω based model provided well matched results with the experimental data. In the computation, the near wall y^+ values were maintained at less than 1.0 for the low-Re near-wall formulation. Figure 9 shows that the comparison between the simulation results and the experimental data shows a good agreement for the overall trends. Here, R is the radial distance from the nozzle axis, and y is the normal distance from the plane.

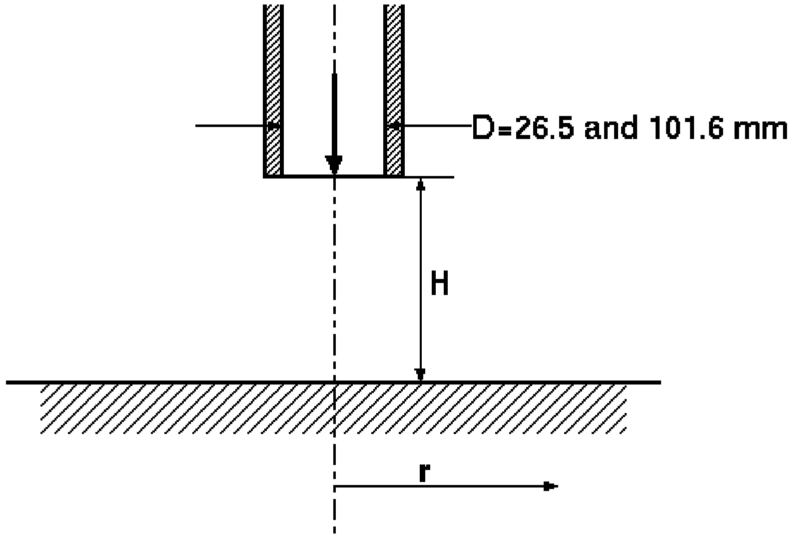

Fig. 7 Experimental Setup

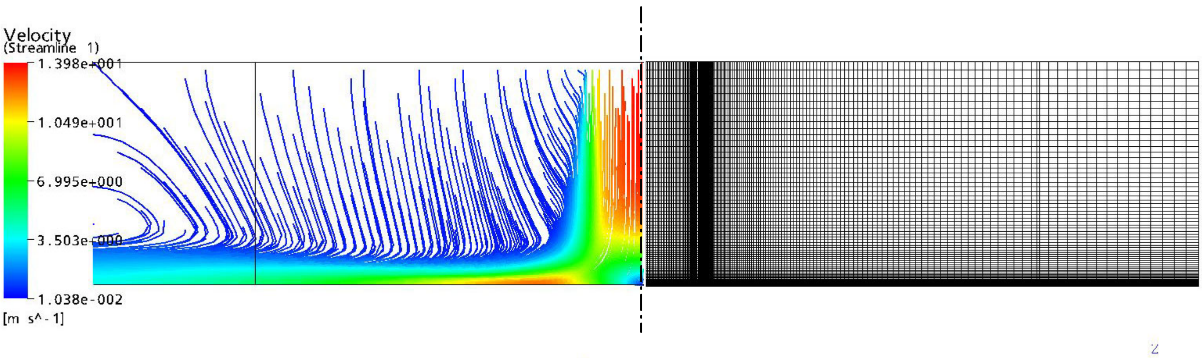

Fig. 8 Meshes and Stream Lines at Re = 70,000 (SST Model)

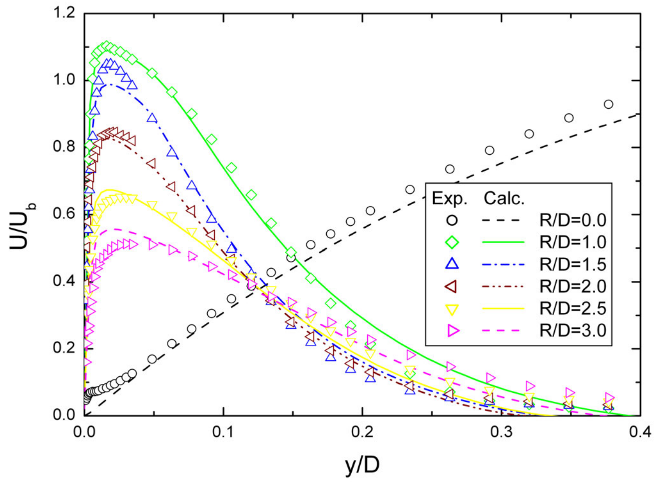

Fig. 9 Stream-wise Mean Velocity Components at Re = 70,000 (SST Model)

3. CANDU MODERATOR INLET NOZZLE

3.1 Simulation Methodology

Each nozzle is connected to a 6" (= 0.1524m) elbow, which is connected to a straight pipe with the same diameter. Moderator passes though a 2m-long pipe, goes into a 90^{o} bend and then it flows into the inlet nozzles. The moderator flow rate of each nozzle assembly is 117.5 L/s, and the *Re* number at the circular pipe is about 1.25×10^{6}. For this high-speed flow, a large number of nodes are required for an accurate computation. Because the memory capacity is limited and different turbulent models are suitable for each flow region, a simulation for each section is performed separately. The interfaces between the domains are carefully selected so as not to disturb the simulation results. The velocity components and the turbulent parameters at the interface are transferred to the inlet boundary conditions of the next flow region.

The hydro-static pressure change was not accounted for and the pressure was assumed to be 1.5 atm, the static pressure at the nozzles. This flow was steady and isothermal. The working fluid was heavy water (D_2O) at 45^{o}C, of which the density was 1084.7 kg/m^3 and the dynamic viscosity (μ) was 8.5×10^{-4} kg/(m$\cdot$s).

3.2 Simulation Results

This section presents the computational results of the straight pipe flow, the 90^{o} curved pipe flow, and the nozzle jets. A half domain is utilized due to the symmetry.

3.2.1 Straight Pipe

For the Re number of $\sim 10^{6}$, the turbulent entrance length is estimated to be 45.7 by equation (2)[6]. The straight pipe is 2-m long, which corresponds to about 26 D, so that the straight pipe flow is not fully-developed. However, the flow was assumed to be fully-developed at the downstream end of the straight pipe for simplicity. Standard k-ε turbulence model was adapted, and the constants of the wall function(Eq. (1)) in the logarithmic region were $\kappa = 0.4$ and B = 5.5 for the circular pipe.

$$\frac{L_e}{d} \approx 4.4\,\mathrm{Re}_d^{1/6} \tag{2}$$

3.2.2 90^{o} Curved Pipe

According to the experimental study of Azzola et al.[3], the existence of a 90^{o} curved pipe affects up to X/D=-2 in the upstream tangent. That is, the measured velocity field at X/D=-2 was in a good agreement with that of the fully-developed pipe flow(data of Laufer[2]). For the simulation of the curved pipe flow in this study, the outlet condition of the straight pipe flow(Section 3.2.1) was applied to the inlet boundary condition at X/D=-2 in the upstream tangent. Figure 10 shows the meshes for the simulation. Structured meshes with 208,229 nodes were generated on the computational domain of the 90^{o} curved pipe section including the upstream straight pipe of $2\times D$. The purpose of the computation in this section was to obtain the flow condition of the curved pipe's outlet which is marked as a blue line in Fig. 10(a). However, unstructured meshes with 8,923 nodes were attached to the outlet of the curved pipe to account for the effect of a downstream pressure distribution. The SSG Reynolds stress model was selected and the y^{+} values of the near-wall cells were 10.0~15.0. Figure 11 shows the streamlines and the velocity field of the secondary flow and Fig. 12 shows the contour of the turbulent kinetic energy on the outlet surface.

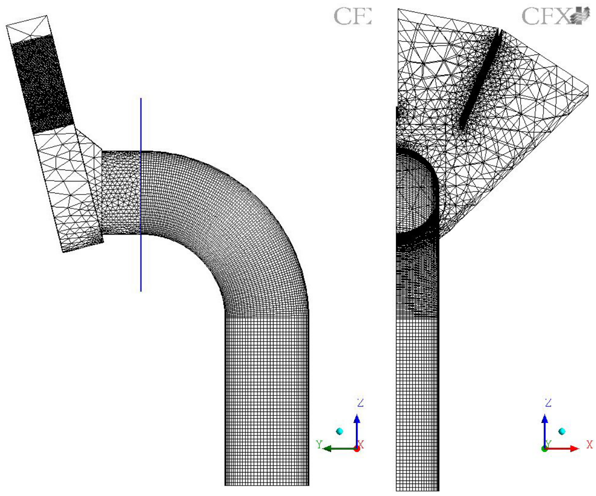

(a) Y-Z Plane View (b) Z-X Plane View

Fig. 10 Mesh Structure for the Bend Calculation

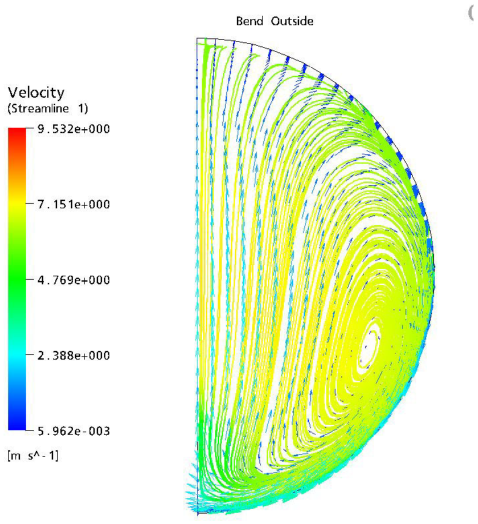

Fig. 11 Surface Streamlines and Tangential Velocity Vectors at the Bend Outlet

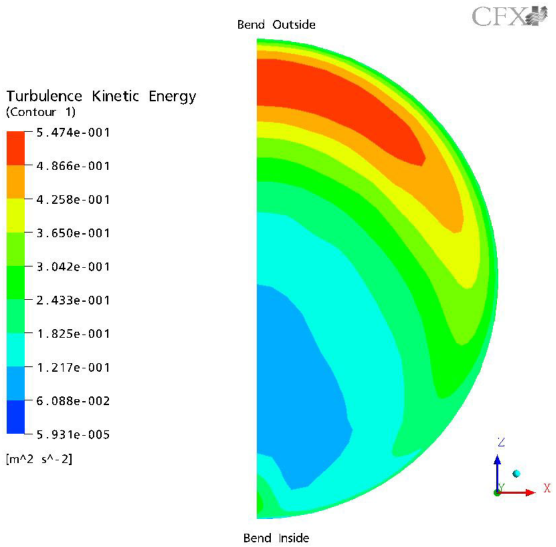

Fig. 12 Turbulence Kinetic Energy at the Bend Outlet

3.2.3 Inlet Nozzle

From the studies of the impinging jets in section 2.3 and Zwart et al.[7], it was acknowledged that the SST k-ω based model was appropriate for the prediction of the impinging jets, and that finer cells were required around the jet boundaries due to the high turbulent dissipation rate. A finer unstructured mesh with 615,379 nodes and a coarser unstructured mesh with 119,073 nodes were generated, including 10 prism layers on the surfaces of the outer walls for the uniform low y^+ values (< 1.0). Figure 13 presents the coarser mesh, where we could confirm higher mesh densities around the jet boundaries. The velocity vectors at the nozzle surfaces are shown in Fig. 14. The nozzle has 4 divided compartments, and the figures show 2 compartments due to the 1/2 computational domain. Especially for the outer compartment, large swirling flows were observed. Figure 15 shows the plots of the velocity magnitudes and the turbulent kinetic energy on the center lines of the nozzle surfaces, which are marked as yellow lines in Fig. 14. As clearly shown in Fig. 15, there were some reversed flows into the nozzles inside each compartment and the turbulent kinetic energy was very low in those “reversed flow” regions.

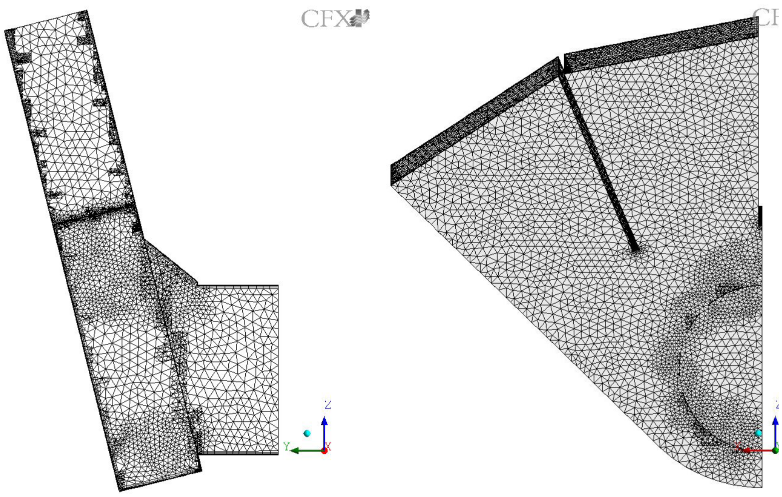

(a) Y-Z Plane View (b) Z-X Plane View (Top View)

Fig. 13 Unstructured Mesh for the Nozzle Calculation

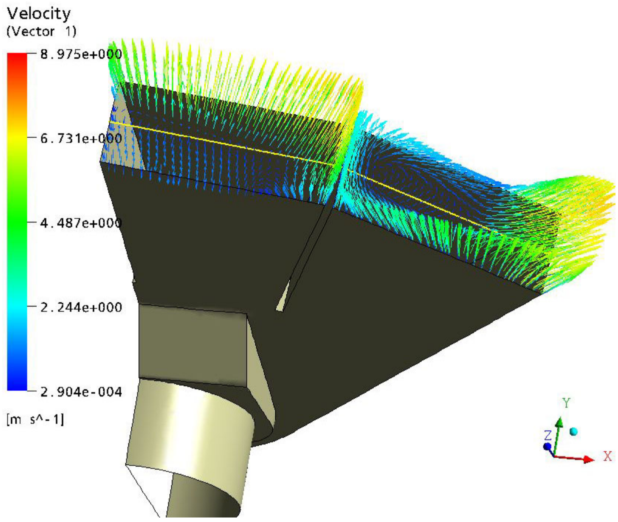

Fig. 14 Velocity Vector at the Nozzle Outlets

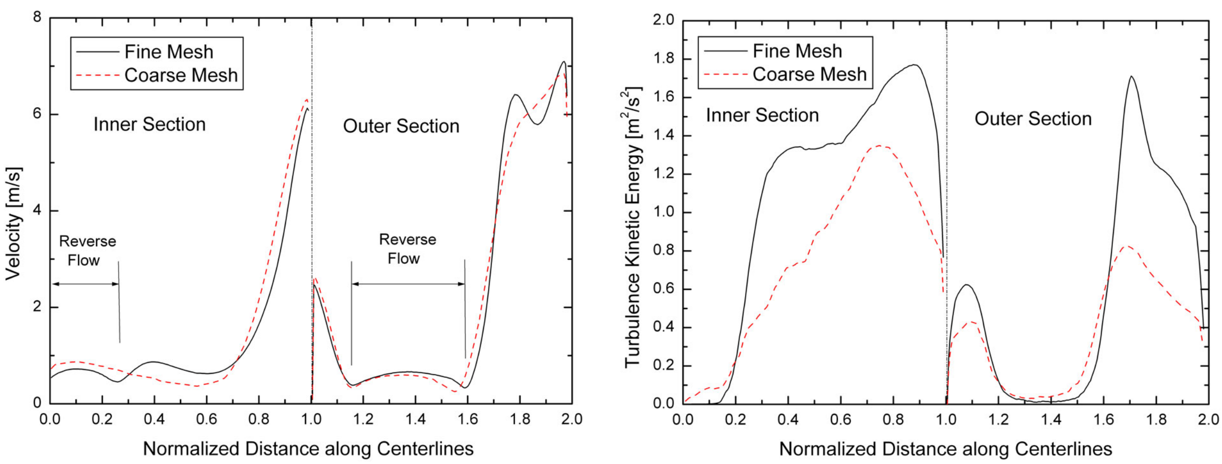

(a) Velocity (b) Turbulence Kinetic Energy

Fig. 15 Simulation Results along the Centerlines on the Nozzle Outlets

4. CONCLUSIONS

For predicting the inlet velocity profile at the CANDU-6 moderator nozzles, a CFD analysis was performed. The selected commercial CFD code was validated against the experimental data of a pipe flow, a curved pipe flow, and impinging jets, which were the major flow types in the moderator nozzle assembly. The straight pipe flow was predicted well by most of the turbulence models. The mean velocities and turbulent parameters of a curved pipe flow were estimated the most closely by the SSG Reynolds Stress model. The SST model was proven to be the most appropriate for the prediction of impinging jets. For the prediction of impinging jets, the accuracy was dependent on the near-wall y^+ values and the local mesh densities.

Based on the validation, the real moderator flow in an inlet nozzle assembly was predicted. To apply proper turbulence models for each flow characteristic, the fluid flow was divided into three computational domains and simulated separately. The simulated data was transferred at the interface between the domains as inlet and outlet boundary conditions. Some reversed flows with a very small velocity magnitude were found at the nozzle surfaces and the flows at the outer compartment were swirling. As a result of the investigation, detailed velocity profiles and turbulent parameters at the nozzle outlets were obtained, which can be applied to the simulation of the CANDU moderator analysis.

ACKNOWLEDGEMENT

This study has been carried out under the nuclear R&D program supported by the Ministry of Science & Technology of the Korean Government. The authors thank Mr. Yong-Kab Lee and other technical assistants in the CFX KOREA co., Ltd. for their valuable advice on using the CFX code.

NOMENCLATURE

d : pipe diameter (m)
L_e : entrance length (m)
U_b : bulk velocity (m/s)
u_τ : friction velocity (m/s)
y : distance from wall (m)
y^+ : non-dimensional distance from wall
τ_w : wall shear stress (Pa)
ν : kinematic viscosity (m^2/s)
ρ : density (kg/m^3)

REFERENCES

(1) *CFX-5: Solver Theory*, ANSYS Canada Ltd., Canada, 1996
(2) J. Laufer, "The Structure of Turbulence in Fully Developed Pipe Flow", NACA Report 1174, 1954.
(3) J. Azzola, J.A.C. Humphrey, H. Iacovides, and B.E. Launder, "Developing Turbulent Flow in a U-Bend of Circular Cross-Section: Measurement and Computation", *Transactions of the ASME*, Vol. 108, June 1986.
(4) C.G. Speziale, S. Sankar, and T.B. Gatski, "Modelling the Pressure-Strain Correlation of Turbulence: an Invariant Dynamical Systems Approach", *J. Fluid mechanics*, Vol. 277, pp 245-272, 1991.
(5) D. Cooper, D.C. Jackson, B.E. Launder, and G.X. Liao, "Impinging Jet Studies for Turbulence Model Assessment, Part I: Flow-field Experiments", *Int. J. Heat Mass transfer*, Vol. 36, pp 2675-2684, 1993.
(6) F.M. White, *Fluid Mechanics*, 3rd Ed., p300, McGraw-Hill Inc., 1994
(7) P.J. Zwart, M. Scheuerer, and M. Bobner, "Free Surface Flow Modelling of an Impinging Jet", *ASTAR Int'l Workshop on Advanced Numerical Methods for Multidimensional Simulation of Two-Phase Flow*, GRS Garching, Germany, Sept. 2003.